

A Pioneering Experimental Study on the Batch Crystallization of the Citric Acid Monohydrate

Enzo Bonacci*

Department of Mathematics and Physics, Scientific High School "G.B. Grassi" of Latina, Latina 04100, Italy

Received: May 12, 2014 / Accepted: June 04, 2014 / Published: June 25, 2014.

Abstract: Citric acid is an important organic substance whose marketing concerns various fields. Nevertheless, until 1997 the scientific literature reported little information about the process of crystallization by cooling through which the commercial product is obtained. In particular, the available studies were aimed to investigate only the kinetics of nucleation and crystal growth neglecting some effective aspects of the industrial crystallization in mechanically stirred apparatus. In order to fill that sci-tech gap, the Department of Chemical Engineering at the University "La Sapienza" of Rome decided to lead a long and meticulous experimental research on the crystallization in discontinuous (batch) of CAM (citric acid monohydrate) in the allotropic form that is stable at room temperature. Due to the number of people involved in that pioneering work, carried out in the historic laboratories of "La Sapienza" (Faculty of Engineering), and motivated by the publication of related M.Sc. dissertations and research papers, such collective effort was called "School of Industrial Crystallization". Among the graduate students in Chemical Engineering that 17 years ago participated in that fruitful experience there was also the author who, under the supervision of Prof. Barbara Mazzarotta, had the specific task of assessing the effects on CAM of changing the crystallization operating conditions until their optimization; the achievements are briefly illustrated in this paper.

Key words: Batch crystallization, CAM, informative essay, crystal size distribution, Zwietering correlation.

1. Introduction

This paper reports the main results of a M.Sc. thesis on the discontinuous (batch) crystallization of the CAM (citric acid monohydrate) written by the author [3] and supervised by Barbara Mazzarotta, who is at the time an Associate Professor of the Faculty of Engineering at the University "La Sapienza" of Rome.

The research started in the spring of 1997, i.e., two decades after the major works on the optimization of the batch crystallization [13, 14], and at least two years before the most important recent papers about it [11, 17].

The importance of such pioneering study to clarify a process about which there was almost an [9, 10, 16, 18] absolute lack of information in the early 1990s literature was acknowledged much later, when it was presented in the 2010 Conference of the Italian

Physical Society [4] and in the 2011 International Year of Chemistry (IYC for short) as invited lecture [5]; then it received the publication honor "Diritto di Stampa" in 2013 [12] and was worthy of two nominations for the prestigious XIII and XIV Sapio Prize for the Italian research [1, 2].

Among the merits, it was the first essay employing not only the physicochemical data on CAM solutions in water by Laguérie et al. [15] but also the formulas established by Bravi and Mazzarotta [6, 7] during that fecund period in the 80's/90's at "La Sapienza" called the School of Industrial Crystallization by the Chemical Engineering Department [8].

The batch cooling crystallization of the CAM was analyzed in differently shaped containers for evaluating the effects of variables such as the shape of the crystallizer's bottom, the intensity of agitation and the conditions of seeding. A series of 20 tests, 15 of which were useful for the dissertation purposes, was

*Corresponding author: Enzo Bonacci, M.Sc. Engineer, research fields: chemistry and chemical engineering. E-mail: enzo.bonacci@liceograssilatina.org.

completed and all the collected data led to the identification of the operating parameters ensuring a good product, i.e., large crystals whose size distribution was homogenous, with no dispersion (the crystal size distribution will be called CSD for brevity).

These conditions can be summarized as follows: agitation speed $\sim 2\%$ above the minimum value for solid suspension; seed crystals large $\sim 10\%$ of the product's desired size; seeding temperature $\sim 0.5\text{ }^{\circ}\text{C}$ over that of spontaneous nucleation; vessel fitted with a round (hemispherical) bottom.

All the pictures come from the original dissertation [3] and their captions in Italian have been kept, being partially translated in the new English captions and explained in the relative paragraphs.

We however remember that the Italian word *prova* means test, *fondo* is bottom, *tondo* is round, *piano* is flat, *conico* is conical, *agitazione* is agitation, *alta* is high, *bassa* is low, *semina* is seed, *leggera* is light and *pesante* translates to heavy.

More similar to the invited talk at the IYC 2011 [5] than to the thesis [3], this expository paper requires a basic knowledge of Chemical Engineering [19].

2. Experiments

2.1 Materials

The experimental equipment was the following:

- #1 Drum of granulated citric acid (50 kg);
- #1 Water distiller;
- #1 Support frame;
- #1 Baffled, jacketed and flat-bottomed glass crystallizer (Fig. 1);
- #1 Baffled, jacketed and round-bottomed glass crystallizer (Fig. 2);
- #1 Baffled, jacketed and conical-bottomed glass crystallizer (Fig. 3);
- #1 Programmable cooling thermostat;
- #1 Agitator from 0 rpm to 2,000 rpm;
- #1 Three-bladed marine propeller;
- #1 Filter funnel;

- #2 Packs of filter paper;
- #1 Vacuum pump and hose;
- #2 Vacuum flasks;
- #2 Anti-hygroscopic ceramic trays;
- #1 Stack of sieves (ASTM series) with shaker;
- #2 Precision electronic scales;
- #1 Optical microscope;
- #1 Professional stopwatch;
- #4 Containers (10 L);
- #2 Beaker flasks (1 L);
- #1 Sheet of waterproof paper (2 m^2);
- #2 Mohr clamps;
- #1 Camera mounted on the microscope eyepiece;
- #2 Glass vessels (5 L);
- #1 Soft hair brush;
- #1 Air compressor;
- #1 Funnel for solids;
- #40 Flasks of 100 mL, 250 mL, 500 mL, 1,000 mL;
- #2 Calibrated scoops;
- #2 Measuring spoons;
- #2 Bottom scraping blades.

2.2 Methods

Since the solubility of citric acid in water increases

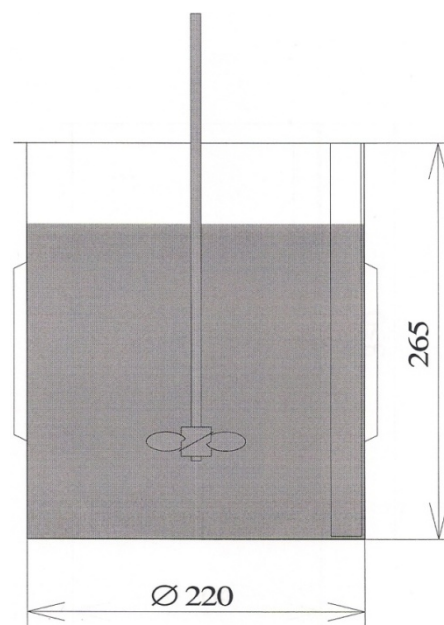


Fig. 1 Flat bottom; $d = 220\text{ mm}$, $h = 265\text{ mm}$.

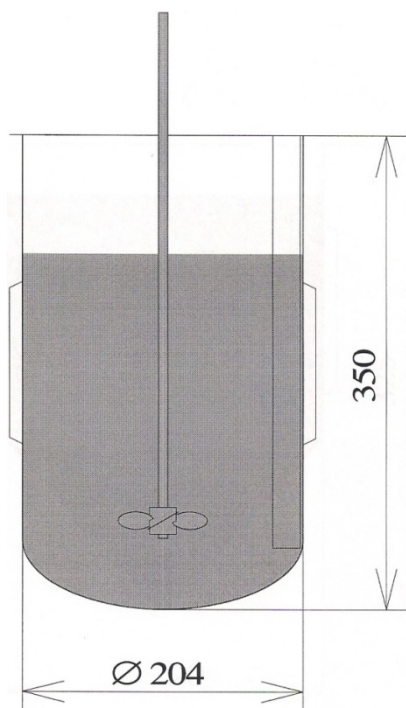


Fig. 2 Round bottom; $d = 204$ mm, $h = 350$ mm.

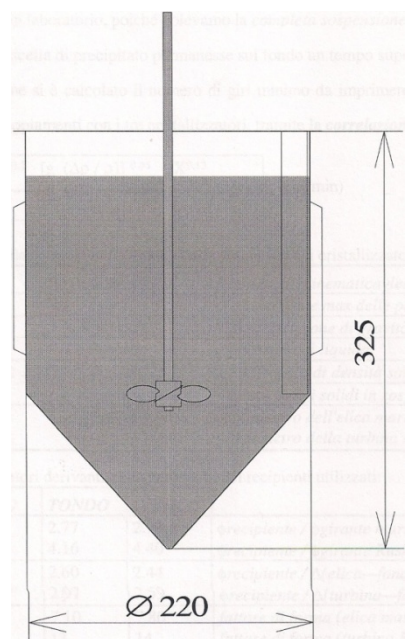


Fig. 3 Conical bottom; $d = 220$ mm, $h = 325$ mm.

significantly with temperature, we considered convenient to crystallize by cooling in order to achieve a supersaturation sufficient for reaching a consistent precipitate and short induction times.

Crystallization trials were performed by varying the agitation intensity, the size and temperature of seeding

in three differently shaped crystallizers with similar volume, each fitted with a cooling jacket.

The effects of these variables on the CSD were evaluated to optimize the operating conditions for producing large CAM crystals with uniform size.

The impact of each operational parameter was then examined individually, looking for an appropriate interpretation of the empirical phenomenology.

The test protocol was executed via the following nine steps:

- (1) Installation of the equipment;
- (2) Preparation of the solution: each test required 3.39 kg of water and 7.09 kg of citric acid, i.e., an aqueous solution of citric acid in the volume of 8 L, saturated at a temperature of 25 °C;
- (3) Solubilization by heating;
- (4) Crystallization by cooling: to attain the desired precipitation, we descended from the temperature of 30 °C to a final temperature between 19 °C and 20 °C, i.e., 5 °C or 6 °C lower than the saturation temperature;
- (5) Separation by under vacuum filtration;
- (6) Drying on exposure to air;
- (7) Classification of the product;
- (8) Analysis through the optical microscope;
- (9) Pictures of some specimens.

2.3 Photographs

The crystal samples were scattered on a slide placed onto the microscope stage (between the objective and the condenser).

After having focused the specimen, we scanned several crystal conformations whose edges reflected the light (bright field illumination) with a distinctive pearly reverb. The direct observation of the samples confirmed the agglomeration intensity and was preparatory to the transposition of the images on film.

We chose six classes showing a good aptitude for the photographic rendering and meeting the following additional requirements:

- (1) They were not contiguous but separated by a

class at least;

(2) They uniformly covered up the CSD spectrum;

(3) The finest-grained class was included as the one with most single crystals;

(4) The coarsest-grained class was excluded for a too wide acronym GSR (grain size range).

For fine-grained classes, the analog camera's exposure time was considerably shortened and the sharpness of the photographs was high (Fig. 4).

It became more difficult to focus on increasing the class size, being sharp only some peripheral areas of the crystal images (Fig. 5).

2.4 Simulation Software

As simulation software we adapted to the CAM the QuickBasic program previously developed for the batch crystallization of potassium sulphate [10, 14].

Since the microscopic analysis of various sized CAM crystals had pointed out their huge tendency to agglomerate, we changed the program routines relative to the nucleation and secondary agglomeration by collision.

The predictions of the new mathematical model were in good agreement with the experimental data and it was possible to reproduce faithfully the influence of the cooling profile on the crystal granulometric properties and the effects of all the operating variables, except the seed size (Section 5.3).

The series of simulation outputs added useful information about both the cooling process and the behavior of the CAM during the batch crystallization.

3. The Geometry Effect

3.1 Description of the Geometry Effect

Far from being equivalent to host the process, the three glass containers played an active role in the crystallization thanks to their differently shaped bottoms.

According to the quality of the crystals produced in the vessels, the round bottom was more efficient than the conical bottom that was better of the flat bottom.



Fig. 4 GSR 355-425 μm , scale 1:50.

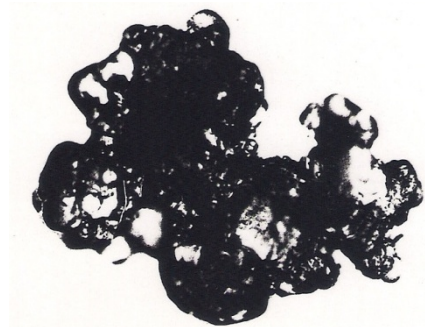


Fig. 5 GSR 0.85-1 mm, scale 1:50.

Such efficiency ranking was a further confirmation to the rule, well-known in industrial practice, to avoid flat bottomed crystallizers.

After having checked the heat exchange efficiency (maximum for the vessel with a conical base, followed by the round and finally the flat bottom), we could reject the hypothesis that the best performance of the round-bottomed container was not due to the shape but to the different thermal profile induced by the cooling jacket.

From the data (Fig. 6), we inferred that the geometry has a marked influence in the two opposite cases of the flat bottom (negative, with a humpback curve) and round bottom (positive, with a swayback diagram). Both of them affected decisively the tests and interfered with the other parameters.

Being in an intermediate position, the vessel with a conical base affected just marginally the tests which were more influenced by other variables.

3.2 Interpretation of the Geometry Effect

The observed effect was explained through complex fluid dynamic considerations related to the vortex flux lines within the three different shapes.

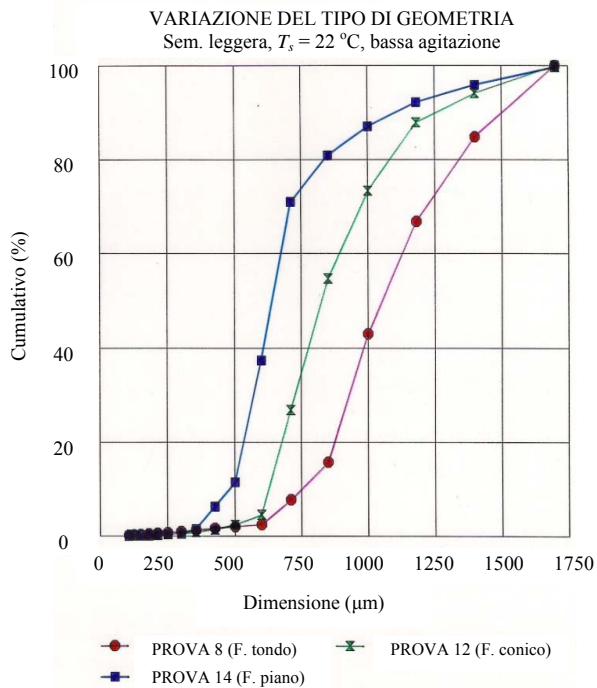


Fig. 6 CSD in differently shaped containers.

We may roughly say that the flat shape broke the flux lines of the solution and suspension (Fig. 7) whereas the two non-linear geometries tended to follow them without big distortions.

The round shape was the best because the flux lines were constantly tangent to its inner surface (Fig. 8).

A connotation of linearity made the conical shape not entirely descending towards the directions of motion induced by the impeller (Fig. 9).

4. The Agitation Effect

4.1 Description of the Agitation Effect

A small and light agitator was placed on top of the crystallizer and it could develop a rotational power of up to 130 W. In addition to reading the rounds per minute (between 0 and 2,000 rpm), its display measured the applied torque in a range between -0.9 and + 99.9 N · cm.

The stirring shaft could not be inserted directly in the gear box because it was an element of instability (going faster than 740 rpm) with off-axis rotations and vibrations increasing in amplitude. In order to absorb the eccentricity of the rotation, avoiding

structural failures and annoying noises, we prolonged the stem of the impeller connecting it to a short metal rod through a flexible and resistant portion of a vacuum hose.

The choice of a three-bladed impeller (marine screw propeller) allowed: energy savings, stability of the rotating system and low background noises.

From the data (Fig. 10), we inferred that a low agitation was preferable to a high speed which, instead, gave bad results with a high percentage of fine-grained

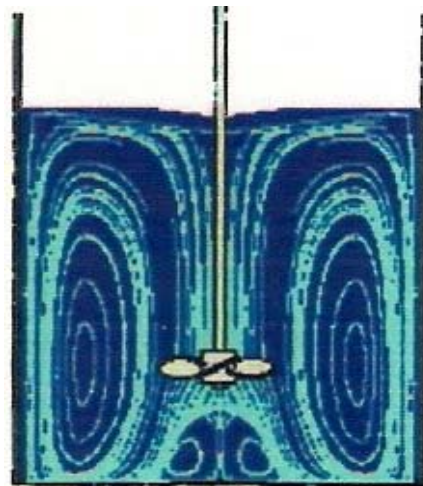


Fig. 7 Simulated flux lines in a flat bottom.

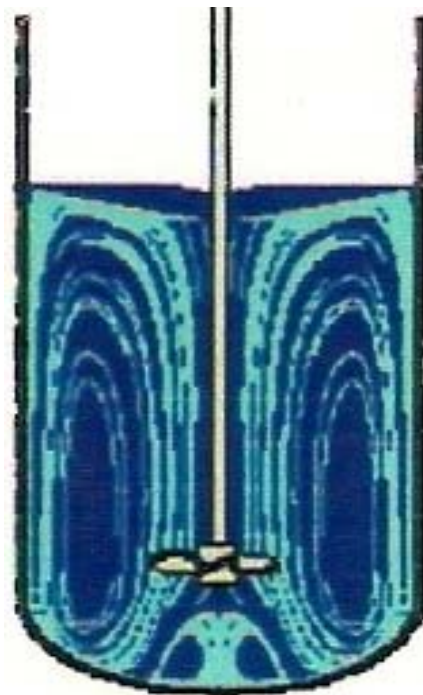


Fig. 8 Simulated flux lines in a round bottom.



Fig. 9 Simulated flux lines in a conical bottom.

crystals, a decrease of the coarse-grained classes and a significantly reduced average size.

The side effects of other impacting parameters, such as light/heavy seeding and flat/round geometry, did not affect the conclusions on the agitation effect because they caused, respectively, a major/minor divergence between the curves or an up/down shift of them.

4.2 Interpretation of the Agitation Effect

We understood that a too high stirring rate favored the secondary nucleation with its absolutely negative effects on the CSD.

The attrition slowed down the crystal growth by splitting agglomerations, but we noticed also another phenomenon: the secondary nucleation by collision, easily recognized for its increase (quadratically with the speed of the impeller).

Then we found that the way to reduce the negative incidences of attrition and secondary nucleation, without renouncing to the benefits of a good mixing, was to maintain the agitation slightly above the just-suspension speed established by the Zwietering correlation [20].

The value we calculated, $N_c \cong 755$ rpm, was 2%

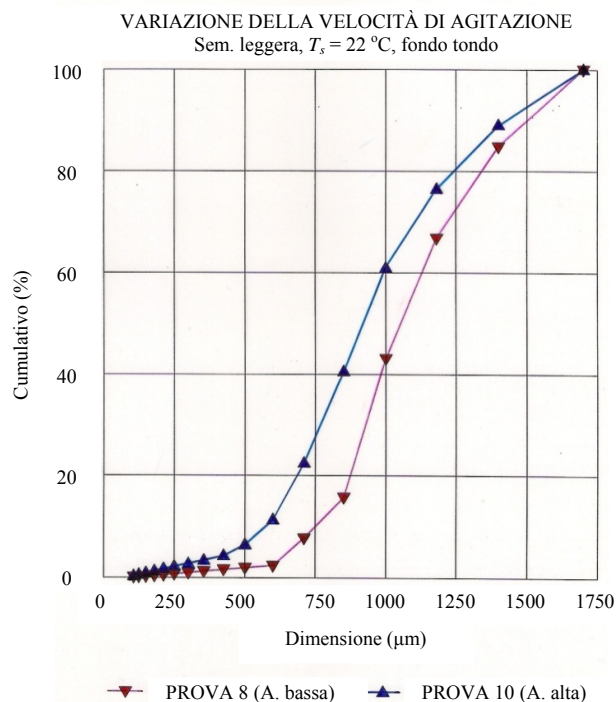


Fig. 10 CSD at different agitation speeds.

above the Zwietering minimum ($N_{JS} \cong 740$ rpm) and it kept the advantages of a supersaturated isotropic homogeneous mixture; it became standard in all tests.

5. The Seeding Effect

We explored the impact of the seed size and quantity on the CSD (Sections 5.1 and 5.2) and we simulated it (Section 5.3); then, we investigated the repercussions of the seeding temperature (Sections 5.4 and 5.5).

5.1 Description of the Seed Size Effect

Once discarded the industrially useless flat bottom (Section 3.1), for comparative diagrams with clearly identifiable curves, we decided to decouple the most influential factors by connecting the heavy seed crystals (HSC for short) to the conical bottom (Fig. 11 – Test 13) and the light seed crystals (LSC for brevity) to the round bottom (Fig. 11 – Test 8).

From the original graphic (Fig. 11), we inferred that a massive seeding augments the risk of a subsequent nucleation whose intensity and duration

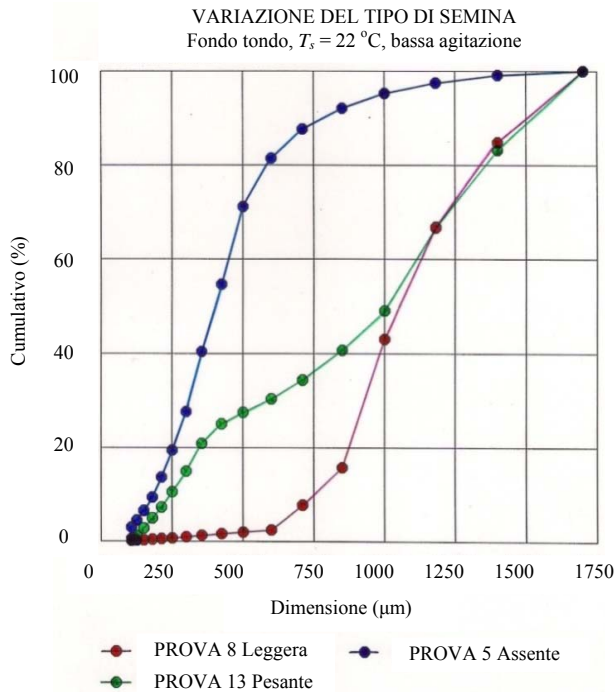


Fig. 11 CSD at different seed sizes.

are directly proportional to both the amount of seed crystals and their average size.

A large CSD with a reduced main peak (seldom turning into a well-defined bimodality) was consequence of the renucleation induced by the HSC (Test 13); the maximum seed size we tested was about half of the expected length: $L_{seed} \approx 1/2 L_{product}$.

Better than the lowest average product size (Fig. 11 – Test 5) due to the absence of seed crystals (acronym ASC), the HSC (Fig. 11 – Test 13) was however unsatisfactory with respect to the optimal situation guaranteed by the LSC (Fig. 11 – Test 8) with the secondary peak dominated by the main bell of the distribution diagram. We found that the perfect seed crystals were large about one tenth of the expected crystal size: $L_{seed} \approx 1/10 L_{product}$.

We also tried medium seed crystals (MSC for short), i.e., $L_{seed} \approx 1/3 L_{product}$, with intermediate results between LSC and HSC.

5.2 Interpretation of the Seed Size Effect

Since the ASC test was the worst of all, we deduced

that seeding had always positive repercussions.

Then, we detected that a less massive seeding was most effective and we explained it on the basis of the supersaturation trend: during the first nucleation the LSC had taken just a minimum part of the available supersaturation; vice versa, the HSC had absorbed the majority of the supersaturation for its own growth.

In the accretion competitive model we developed, the LSC (with a surface/volume ratio greater than for the HSC) was expected to consume a considerable share of the remaining driving force; it had the dual effect of increasing the average size of the product and keeping the level of super saturation below the secondary nucleation threshold.

With the LSC, we reached an almost perfect Gaussian distribution for, as we interpreted it, its almost total participation in the crystal generation and the consequent positive abatement of the driving force.

The crystal generation was instead strongly inhibited by the HSC for the successive waves of nucleation due to the rather high residual driving force.

In our mechanism, the HSC were disadvantaged in supplying the energy for their low ratio surface/volume, so the growth focused on small crystals penalizing the final CSD.

A further reason for preferring the LSC was that it had little impact on the solution, whereas the HSC exerted a greater influence on the tests which were too similar to each other and insensitive to the other parameters.

5.3 The Limits of the Simulation Program

As mentioned in Section 2.4, a program in QBasic was used to simulate all the experimental evidence and it worked pretty well until we tried to reproduce the seed effect on the CSD (Fig. 11) with the unsatisfactory result shown in Fig. 12: the curves that simulated LSC (Test 12) or ASC (Test 5) were adequate but the curve simulating HSC showed a big

discrepancy with Test 9.

A plausible explanation for this failure, i.e., the abnormal overestimation of the fine-grained crystals, lay in the strong tendency to agglomerate manifested in all the CAM granulometric classes.

Although we tried to better the QBasic program through subroutines modeling the GSR-independent agglomeration tendency of the CAM, we could not go beyond the graph of Fig. 12 (our best achievement) because a further improvement of the central curve (Test 9) would have meant a deterioration in both the other two curves (Tests 5 and 12) and in the predictions about the other tests.

5.4 Description of the Seeding Temperature Effect

Three successive temperatures of seeding were tested: 24, 23 and 22 °C.

We had the best product at the lowest temperature (22 °C) and, on the other hand, the worst result at the highest temperature (24 °C).

Our attempt to diminish the seeding temperature to 21 °C failed because the system nucleated in an interval between 21.4 °C and 21.7 °C; such tests were invalidated but they were however useful to assure us that, at our operational conditions, $T = 22$ °C was the lowest integer value before the spontaneous nucleation, i.e., the temperature below which we could not seed.

From the experimental evidence summarized in Fig. 13, we detected a net improvement of the crystalline product when seeding at low temperature, obviously before the nucleation.

We found that the best temperature to seed was slightly above the spontaneous nucleation temperature; in fact, when we seeded much above such threshold our product deteriorated.

We noticed that it was meaningless to seed when the nucleation had already taken place and the tests carried out in this manner were invalidated.

All data collected showed the effects of a gradual change in the temperature of seeding, albeit more

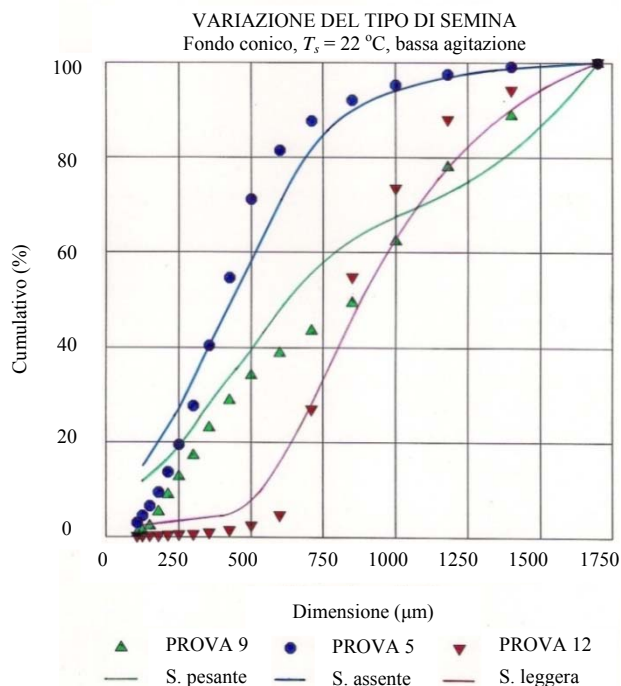


Fig. 12 Simulated CSD at different seed sizes.

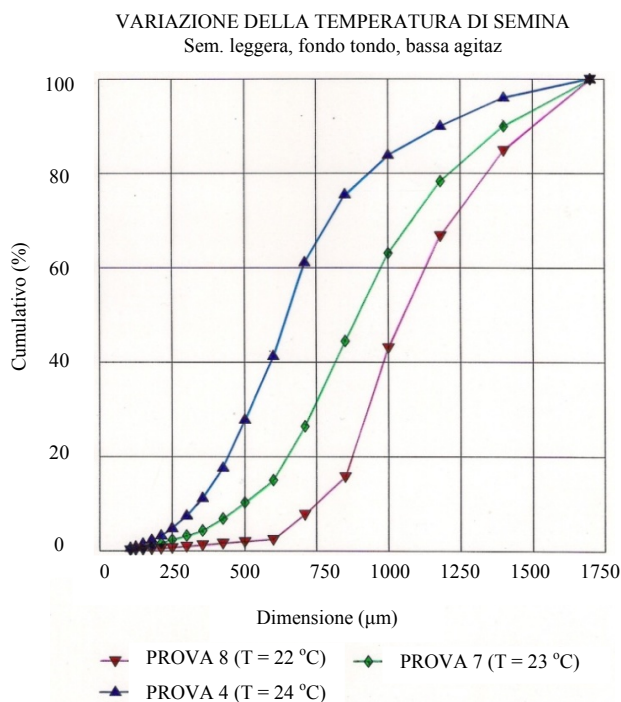


Fig. 13 CSD at different seeding temperatures.

evidently in tests where we chose the LSC (well separated curves) than those with HSC (tight curves).

5.5 Interpretation of the Seeding Temperature Effect

We discovered that the seeding effect was much

more effective when the addition of the seed crystals was close to the nucleation temperature (at which, in the absence of seeding, there is spontaneous precipitation of the supersaturated solution). Vice versa, when we seeded at a much higher temperature, we obtained a bad crystalline product.

The best interpretation was that when seeding at a high thermal level, with a still strong metastability, we perturbed the meta-equilibrium accelerating its end as a consequence of the low initial supersaturation and of the tiny residual seed.

6. Conclusions

Fully described in the 1998 M.Sc. thesis of the author [3], a series of experiments on the batch crystallization of CAM from aqueous solutions, conducted at the laboratories of “La Sapienza” (Faculty of Engineering) familiarly known as “St. Peter in Chains” (from the close famous Church in Rome), led to the following general conclusions:

(1) The industrial practice to use round-bottomed or conical-bottomed crystallizers, discarding those flat-bottomed, is grounded on mechanical strength reasons and justified by the nature of the process: the flat geometry is inadequate for a quality product whereas the convex bottom, more than the conical one, is better to attain large sized homogeneous crystals.

(2) Seeding is always positive but the LSC (particularly $L_{seed} \approx 1/10 L_{product}$) is better than the MSC which is, in turn, more effective than the HSC, augmenting the seed size we increase the risk of a secondary nucleation which would spoil the CSD.

(3) The best temperature to seed is just above the spontaneous nucleation temperature because far from this threshold both the homogeneity and the average size of the product decrease; it does not make any sense to add seed crystals when the nucleation has already occurred.

(4) The best agitation speed is the minimum that ensures the suspension of the particles from the bottom of precipitate in the crystallizer; although

giving incorrect information for geometries different from the flat shape, the Zwietering correlation is, however, essential for determining the limit speed.

(5) The experimental work was supplemented by a QBasic program to simulate both the CSD and the supersaturation trend; it fails with the HSC.

Since we have given a brief sketch of an elaborate old work avoiding calculations, there will presumably follow further papers expounding the computational aspects here neglected.

Acknowledgments

The author thanks the Organizing Committee of the IYC 2011, in particular, the Chairman Francesco Giuliano, for the invitation to lecture and the Academy of the Sapio Prize for the invitations to the XIII and XIV awarding ceremonies.

References

- [1] Ausili, M. *The First Pontine Nomination to the Sapio Prize of Enzo Bonacci in 2008*. Latina in Vetrina Home Page. www.latinainvetrina.it/content/la-primacandidatura-pontina-al-premio-sapio-del-prof-enzo-bonacci-nel-2008 (accessed July 8, 2013).
- [2] Ausili, M. *Enzo Bonacci at the XIV Sapio Prize Awarding Ceremony on 2014-02-18*. Latina in Vetrina Home Page. www.latinainvetrina.it/content/il-prof-enzo-bonacci-alla-cerimonia-conclusiva-del-xiv-premio-sapio-il-18022014 (accessed March 7, 2014).
- [3] Bonacci, E. *Experimental Study on the Crystallization of the Citric Acid*. M.Sc. Dissertation, The University of Rome “La Sapienza”, 1998.
- [4] Bonacci, E. *Experimental Survey on the Batch Crystallization of CAM*, In Proceedings of the XCVI Conference of the Italian Physical Society (Atticon5594 Va-C-2), Bologna, 2010.
- [5] Bonacci, E. *Experimental Survey on the Batch Crystallization of CAM*, In Proceedings of the International Year of Chemistry (IYC 2011), Latina, 2011. The Liceo Scientifico Statale “Giovanni Battista Grassi” of Latina Home Page. http://grassi.deltaeffe.it/images/modulistica/archivio/fisica/Cristallizzazione_in_discontinuo_dell'acido_citrico_Prof_Enzo_Bonacci.pdf (accessed April 30, 2011).
- [6] Bravi, M.; Mazzarotta, B. *Primary Nucleation of Citric Acid Monohydrate: Influence of Selected Impurities*.

- Chem. Eng. Journal* **1998**, 70(3), 197-202.
- [7] Bravi, M.; Mazzarotta, B. Size Dependency of Citric Acid Monohydrate Growth Kinetics. *Chem. Eng. Journal* **1998**, 70(3), 203-207.
- [8] Bravi, M. Preface of the Experimental Study on the Crystallization of the Citric Acid. The Aracne Editrice Home Page. www.aracneeditrice.it/pdf/9788854857674.pdf (accessed Jan 15, 2013).
- [9] Chianese, A.; Di Cave, S.; Mazzarotta, B. Main Factors Influencing the Crystal Size Distribution from a Batch Cooling Crystallizer. *Crys. Res. Technol.* **1986**, 21, 31-39.
- [10] Chianese, A.; Di Cave, S.; Mazzarotta, B. Crystallization Kinetics of Potassium Sulphate in an MSMR Cooling Crystallizer. *Quad. Ing. Chim. Ital.* **1987**, 23(6), 8-13.
- [11] Chung, S.; Ma, D.; Braatz, R. Optimal Seeding in Batch Crystallization. *Can. J. Chem. Eng.* **1999**, 77, 590-596.
- [12] Giuliano, F. *An Examination of the Experimental Study on the Crystallization of the Citric Acid Monohydrate (CAM) by Enzo Bonacci*. The Università Politecnica delle Marche Home Page. <http://educa.univpm.it/apptec/2013bona.html> (accessed Apr 3, 2013).
- [13] Jones, A.; Mullin, J. Programmed Cooling Crystallization of Potassium Sulphate Solutions. *Chem. Eng. Sci.* **1974**, 29(1), 105-118.
- [14] Jones, A. Optimal Operation of a Batch Cooling Crystallizer. *Chem. Eng. Sci.* **1974**, 29(5), 1075-1087.
- [15] Laguérie, C.; Aubry M.; Couderc, J. P. Some Physicochemical Data on Monohydrate Citric Acid Solutions in Water: Solubility, Density, Viscosity, Diffusivity, pH of Standard Solution, and Refractive-Index. *J. Chem. Eng. Data* **1976**, 21, 85-87.
- [16] Laguérie, C.; Muratet, G.; Angelino, H. Choosing a Method for Determining the Velocity of Crystal Growth in a Fluidized Bed: Application to the Growth of the Acid Crystals. *Chem. Eng. Journal* **1977**, 14, 17-25.
- [17] Lang, Y.; Cervantes, A.; Biegler, L. Dynamic Optimization of a Batch Cooling Crystallization Process. *Ind. & Eng. Chem. Res.* **1999**, 38, 1469-1477.
- [18] Nývlt, J. *Industrial Crystallization: The State of the Art*, 2nd ed.; Verlag Chemie: Weinheim, 1982.
- [19] Perry, R. H.; Green, D. W. *Perry's Chemical Engineers' Handbook*; McGraw-Hill: New York, 2007.
- [20] Zwietering, T. N. Suspending of Solid Particles in Liquid by Agitators. *Chem. Eng. Sci.* **1958**, 8, 244-253.